

Triplet Formation by Charge Recombination in Thin Film Blends of Perylene Red and Pyrene: Developing a Target Model for the Photophysics of Organic Photovoltaic Materials

René M. Williams*[†], Nguyễn Văn Anh^{†§} and Ivo H. M. van Stokkum[‡]

[†]*Molecular Photonics Group, van't Hoff Institute for Molecular Sciences (HIMS), Universiteit van Amsterdam, Science Park 904, 1098 XH Amsterdam, The Netherlands and* [‡]*Department of Physics and Astronomy, Vrije Universiteit, de Boelelaan 1081, 1081 HV Amsterdam, The Netherlands*

[§]*current address: Department of Physical Chemistry, School of Chemical Engineering, Hanoi University of Science and Technology, No1 Dai Co Viet Road, Hanoi, Vietnam.*

Supporting information

content

Figure S1, UV-Vis absorption spectra of films and compounds in solution	S4
Figure S2, Fluorescence spectra of films and compounds in solution	S5
Figure S3, Femtosecond spectra with fit from global target analysis of PDI-Py with selection of kinetic traces of the PDI-Py film, data and fit at specified wavelengths and Target analysis of PDI-Py mixed film blend	S6
Figure S4 Global target analysis of PCBM-P3HT film with description	S9
Figure S5 Target analysis scheme for PCBM-P3HT film	S11
Figure S6 fs-TA data-matrix obtained for PCBM-P3HT	S12
Figure S7 Comparison with ground state bleaching spectrum of Riedle et al. for the PCBM-P3HT long lived polaron state	S13
Samples and preparation	S14
Spectroscopy	S15
Layer thickness	S16
Global and Target Analysis using Glotaran	S17
Target analysis of PDI only film	S19

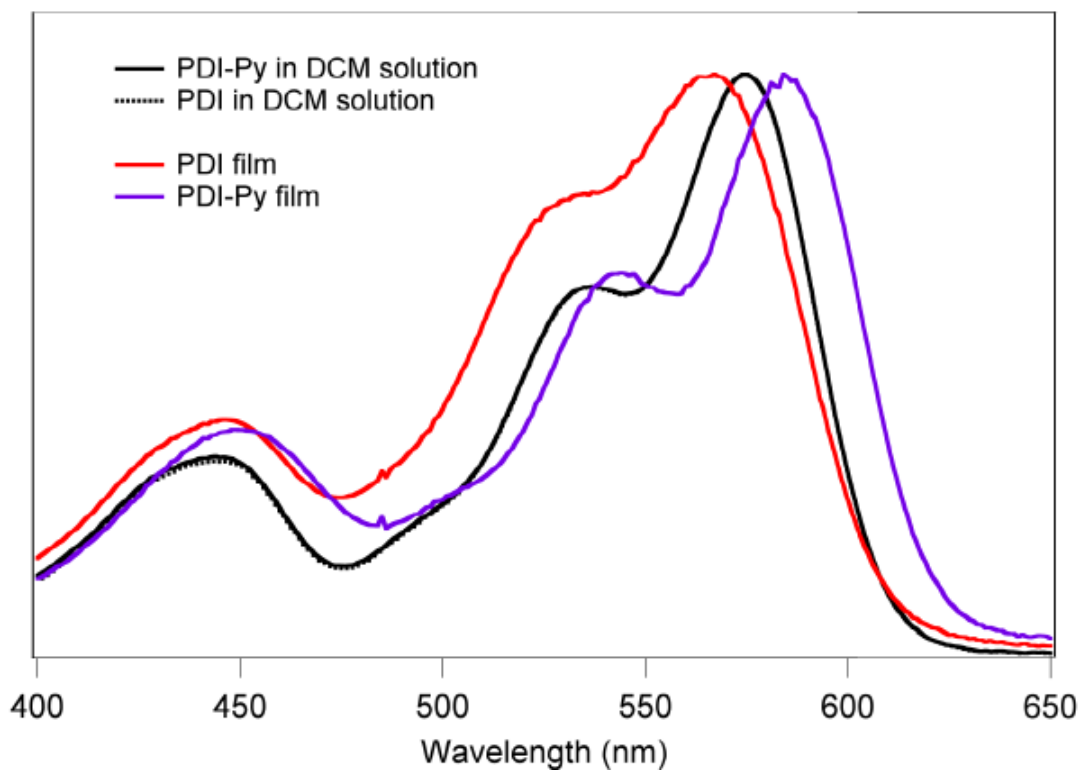


Figure S1. Comparison of the UV-Vis absorption spectra of the two films and of the solutions of the components in dichloromethane (DCM). Note that the two spectra in solution, of **PDI** and of the mixture **PDI-Py**, overlap perfectly.

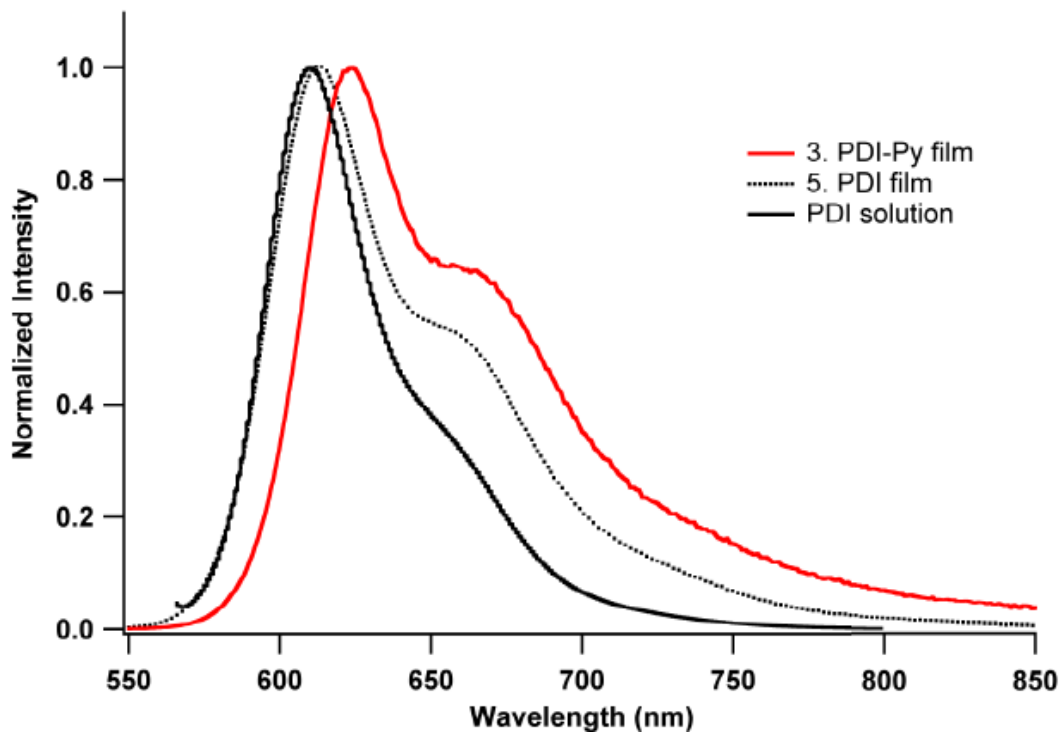


Figure S2. Emission spectra of the two films compared to that of **PDI** in solution.

Target analysis of PDI-Py mixed film blend
Selection of spectra of the PDI-Py film, data and fit at specified times.

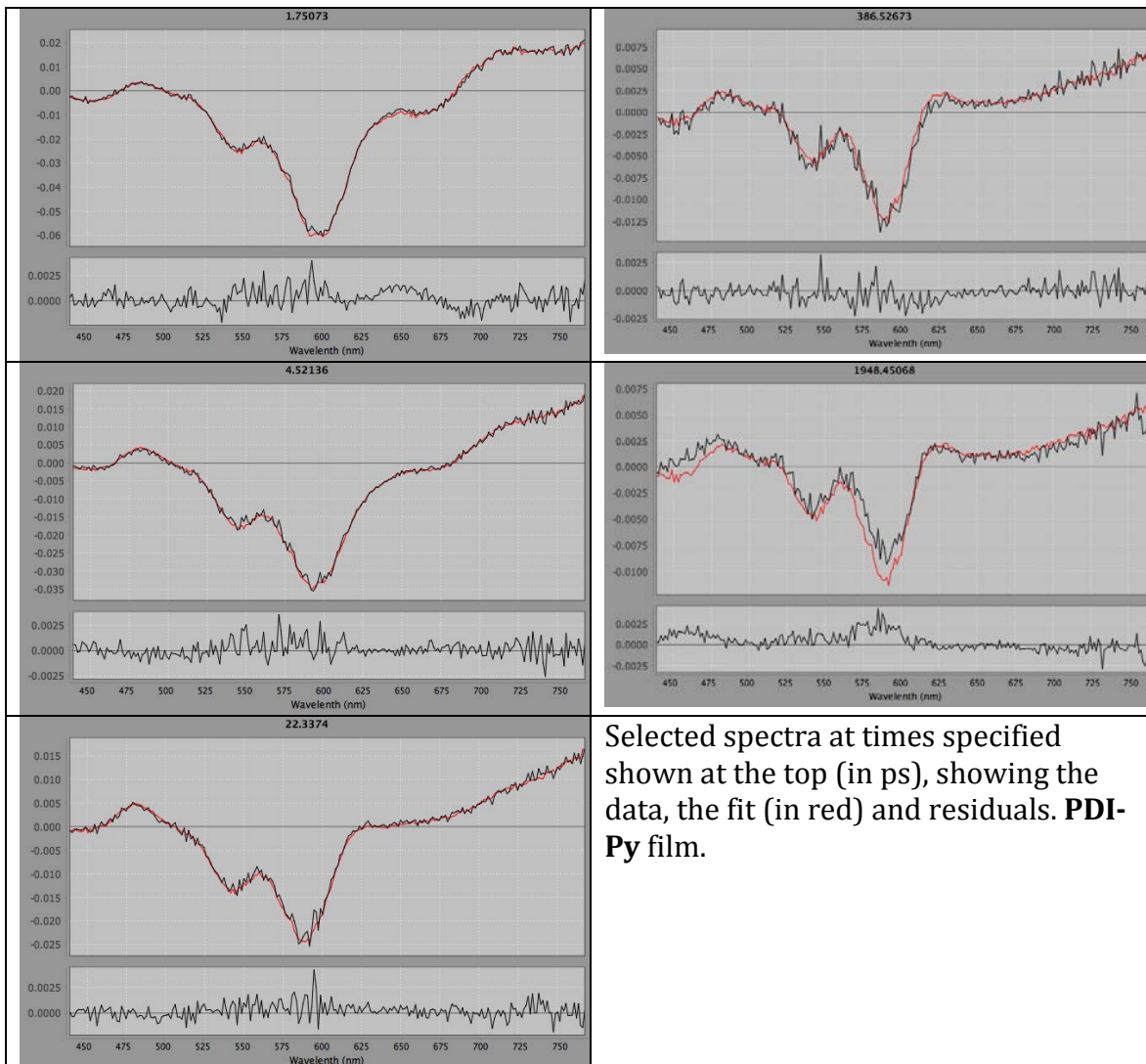
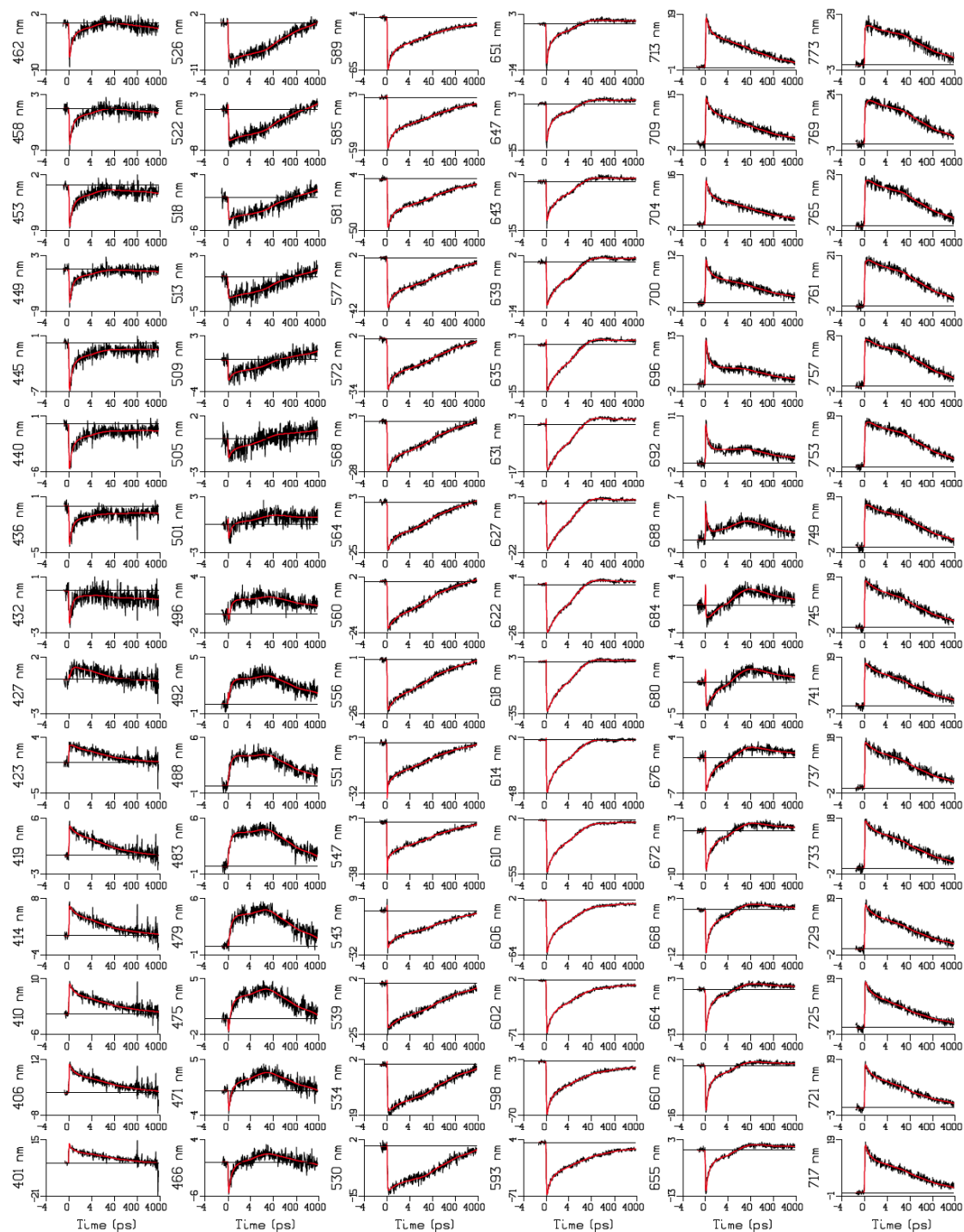


Figure S3. Selected spectra at specific times with fit from target-analysis of **PDI-Py**.

Selection of kinetic traces of the PDI-Py film, data and fit at specified wavelengths



Selected measured (black) and fitted (red) time traces of TA data of the **PDI-Py** film. The probe wavelength is written as ordinate label. Time axis is linear from -4 till 4 ps, relative to the location of the IRF maximum, and logarithmic thereafter.

Output data of target analysis from TIMP/Glotaran. PDI-Py film.

Information about the K-matrix and equality of spectra used within the target analysis. **PDI-Py** film.

K-matrix (rate constants [10^{12} s^{-1}]),

		from						
	A (0.40)	B (2)	C (11)	D (18)	E (211)	F (~5808)	G (~81762)	
to	A	-2.494	0	0	0	0	0	0
	B	1.243	-0.5201	0	0	0	0	0
	C	0	0.2137	-0.9369E-01	0	0	0	0
	D	0.9493	0.4740E-02	0.9354E-01	-0.5556E-01	0	0	0
	E	0	0	0	0.1806E-01	-0.4719E-02	0	0
	F	0	0	0	0.1684E-01	0	-0.1722E-03	0
	G	0	0	0	0.1036E-01	0.4782-06	0.7218E-04	-0.1223E-04
	GS	0.302	0.302	1.5E-3	10.3E-03	0.4718E-02	0.1000E-03	0.1223E-04

The diagonal elements represent the (negative) of the sum of all rates. The negative rates incorporate the reaction to the ground state. The rate to the ground state is also indicated as the last row (**GS**).

The lifetimes of the species (in ps) are indicated in the top row between brackets.

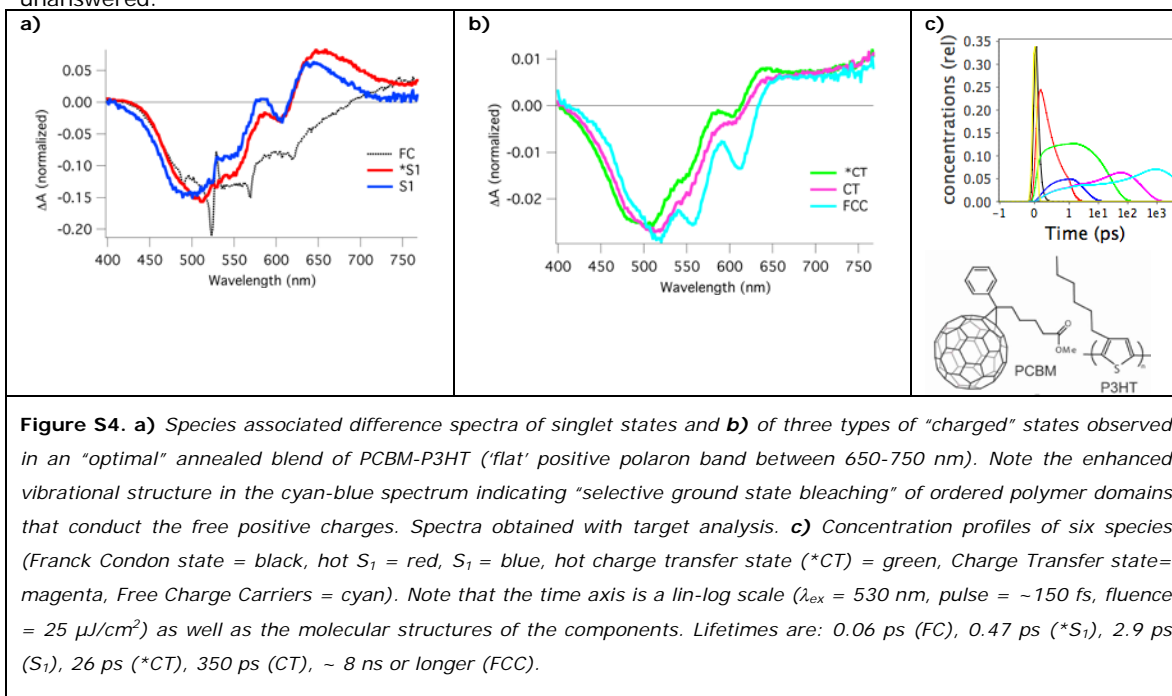
Spectral equivalence was assumed for B and C, and for D, E and F.

For G, a spectral zero constraint was used above 700 nm.

The lifetimes of F and G are on the limit of our detection time domain (3.4 ns) and thus are prone to a larger error.

PCBM-P3HT

Conjugated polymer based organic photovoltaics (OPVs) have been the subject of intense investigation over the past decade, as the promise of flexible, large-area cells processed using low-cost printing techniques could allow them to compete with more established semiconductor technologies.¹ A major breakthrough was achieved by using bulk heterojunction (BHJ)² structures, wherein the active layer is spin-coated from a mixed solution of photo-activated donor and acceptor materials. The function of such conjugated polymer solar cells is based on photoinduced electron transfer from a donor to an acceptor. Among the organic photovoltaics, the polymer–fullerene composite solar cells are most ubiquitous, because fullerenes have their high electron affinity and ability to transport charge effectively.³ Especially the composited blends with regioregular poly(3-hexylthiophene) (RR-P3HT) and the [6,6]-phenyl-C₆₁ butyric acid methyl ester fullerene derivative, (PCBM) have emerged as prototypical photovoltaic systems (PCBM:P3HT) as applied in Konarka's (first generation) organic solar cells² with a power conversion efficiency (PCE) ~ 5%, depending on the regio-regularity and molecular weight of the polymer.⁴ This most extensively used and studied combination of materials still poses some intriguing questions. Although many studies have appeared in the last two years on these blends, still many questions remain unanswered.



Femtosecond transient absorption measurements have shown extensive sharpening of the ground state bleaching signals of the polythiophene polarons in time (See figure S4) showing multistep charge transport towards more ordered regions of the polymer within the first 3 ns (in BHJ PCBM/P3HT blends). Our results indicate that we can spectrally discriminate the Coulombic bound electron hole-pair and the free charge carriers (that reside in more ordered polymer regions). A broad unstructured ground state bleaching signal shows geminate charge recombination occurring preferentially in amorphous regions on a 350 ps timescale. Extensive analysis of the FTA data-matrix using a target model with 6 excited state species playing a role within the first 3 ns shows clear fingerprints of all excitonic and polaronic states (see figure S5). Our results are also in agreement with the current concept that triplet charge recombination does not occur in this material as the triplet state of both components (1.5 eV for PCBM [absorbing at 760 nm] and 1.4 eV for RR-P3HT [absorbing at 700 nm]) are above the energy level of the geminate polaron pair or charge transfer states.

¹ *Organic Photovoltaics: Materials, Device Physics, and Manufacturing Technologies*, Brabec, C. J.; Dyakonov, V.; Scherf, U. Eds. Wiley-VCH Verlag GmbH & Co. KGaA: Weinheim, **2009**.

² Yu, G.; Gao, J.; Hummelen, J. C.; Wudl, F.; Heeger, A. J. *Science* **1995**, *270*, 1789.

³ Thompson, B.C., Frechet, J. M. J. *Angew. Chem. Int. Ed.* **2008**, *47*, 58 –77.

⁴ Li, G., Shrotriya, V., Huang, J., Yao, Y., Moriarty, T., Emery, K., Yang, Y. *Nature. Mater.* **2005**, *4*, 864–868.

These data shed light on the conflict between Moses⁵ and Österbacka⁶ on the charge generation mechanism (see also discussion in ref 7), supporting the mechanism proposed by Moses, but also introducing an extra step.

Combined with an extensive Global and Target analysis the femtosecond spectroscopy gives us a valuable tool to resolve fundamental questions regarding the 'primary events' in organic photovoltaics. Three spectrally and kinetically different charged species are extracted from our data by using analysis methods that are mainly applied in the bio-physics community.⁸

⁵ Hwang, I. W.; Moses, D.; Heeger, A. J. *J. Phys. Chem. C* **2008**, *112*, 4350

⁶ Osterbacka, R.; An, C. P.; Jiang, X. M.; Vardeny, Z. V. *Science* **2000**, *287*, 839; (b) Westerling, M.; Osterbacka, R.; Stubb, H. *Phys. Rev. B* **2002**, *66*, 165220; (c) Aarnio, H.; Sehati, P.; Braun, S.; Nyman, M.; de Jong, M. P.; Fahlman, M.; Österbacka, R. *Adv. Energy Mater.* **2011**, *1*, 792-797.

⁷ Clarke, T. M., Durrant, J. R. *Chem. Rev.* **2010**, *110*, 6736–6767.

⁸ (a) Zhu, J. Y.; Gdor, I.; Smolensky, E.; Friedman, N.; Sheves, M.; Ruhman, S., *J. Phys. Chem. B* **2010**, *114*, 3038-3045; (b) Savolainen, J.; Dijkhuizen, N.; Fanciulli, R.; Liddell, P. A.; Gust, D.; Moore, T. A.; Moore, A. L.; Hauer, J.; Buckup, T.; Motzkus, M.; Herek, J. L., *J. Phys. Chem. B* **2008**, *112*, 2678-2685; (c) van Stokkum, I. H. M.; Larsen, D. S.; van Grondelle, R., *Biochim. Biophys. Acta - Bioenerg.* **2004**, *1657*, 82-104; (d) Muller, M. G.; Drews, G.; Holzwarth, A. R., *Biochim. Biophys. Acta* **1993**, *1142*, 49-58; (e) Holzwarth, A. R.; Schatz, G.; Brock, H.; Bittersmann, E., *Biophys. J.* **1993**, *64*, 1813-1826; (f) van Wilderen, L. J. G. W.; Lincoln, C. N.; van Thor, J. J., *PLoS One* **2011**, *6*, e17373.1-14; (g) Roelofs, T. A.; Lee, C. H.; Holzwarth, A. R., *Biophys. J.* **1992**, *61*, 1147-1163; (h) <http://glotaran.org/>

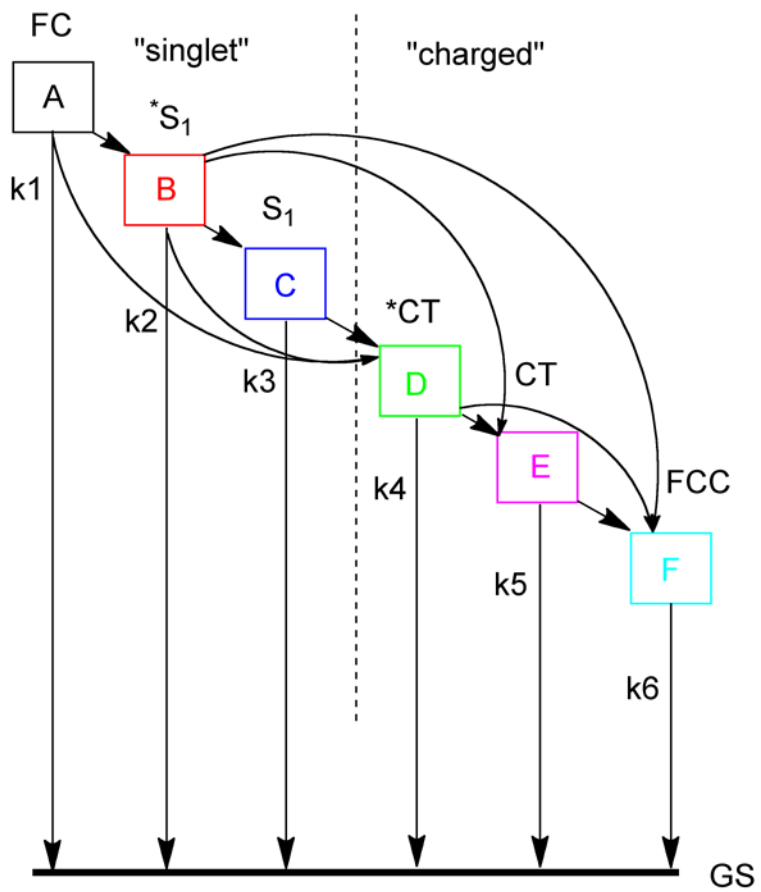


Figure S5 Target analysis scheme used for PCBM-P3HT.

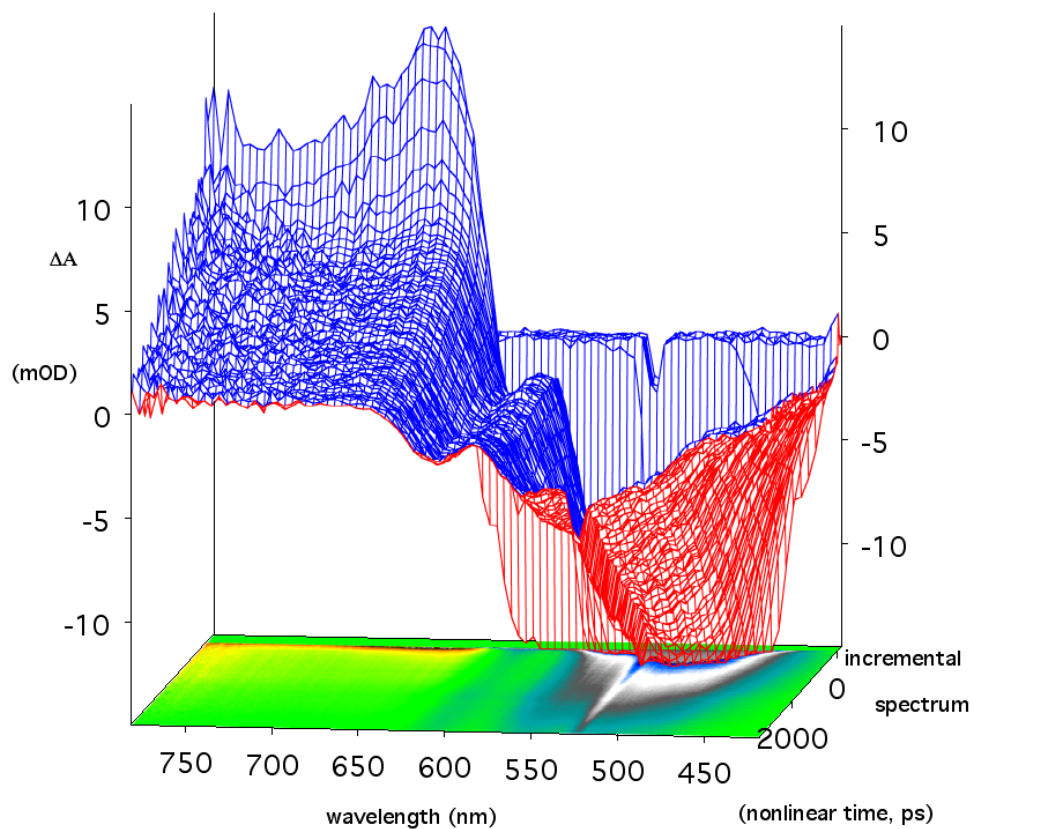


Figure S6. Raw data matrix showing the femtosecond transient absorption data of the PCBM/P3HT film. Note that the “time zero” starts in the back of the 3D plot. Wavelength increases to the left. See figure S4 for details.

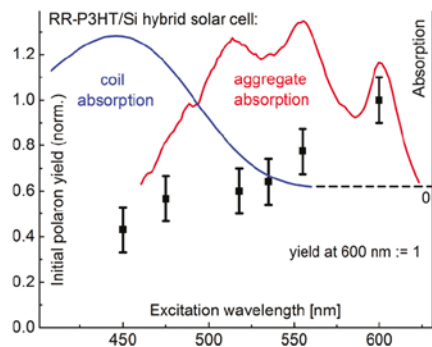


Figure 9. Dependence of initial polaron yield (black squares) on excitation wavelength for RR-P3HT/Si heterojunctions. Selective excitation of coiled (blue curve) vs aggregated (red curve) RR-P3HT domains reveals greater than a factor of 2 more efficient charge separation if exciting directly the aggregated RR-P3HT domains.

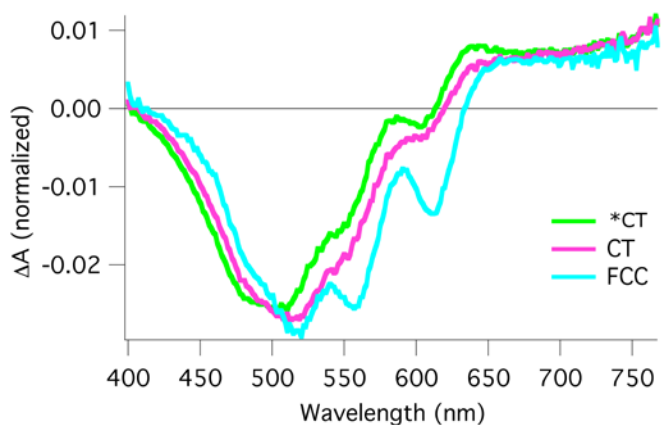


Figure S7. Comparison of the (inverted) ground state bleaching spectrum (related to singlet formation by red-edge excitation of neat P3HT films reported by Riedle et al. (red curve in top picture) with the ground state bleaching obtained here by target analysis of PCBM-P3HT blend (cyan-blue curve in lower picture). The cyan-blue signal in the lower picture is related to positive charges in the blend film (free charge carriers). *Top picture is reprinted with permission from: J. Am. Chem. Soc. 2011, 133, 18220– 18233.*

Copyright 2011 American Chemical Society.

Samples and preparation

Perylene Red (**PDI**) from Exciton Inc, pyrene from Aldrich ($\geq 99.0\%$), and spectroscopic-grade solvents were used as received.

The thin film samples were prepared by spin coating (1600 rpm) from dichloromethane solutions (15 mg **PDI**/ml) on quartz substrates (with a Delta 10TT spincoater, *BLE Laboratory Equipment GmbH*). For the thin film blend (15 mg **PDI** + 12.85 mg **Py**)/ml) was used. The obtained samples were stored at room temperature for several days before experiments were performed. Before the coating processes, all solutions were filtered (0.4 μm PVDF HPLC filters) to remove aggregated particles. The quartz substrates were immersed in potassium permanganate in concentrated sulphuric acid solution for several days to remove all trace of resin or organic matter, and then washed with hydroperoxide solution in acidic medium (using hydrochloric acid) ($\text{H}_2\text{O} : \text{H}_2\text{O}_2 \text{ 30\%} : \text{HCl 35\%} = 4:1:1$) to remove manganese dioxide traces. After being washed with demi water, they were rinsed with acetone, then with ethanol and dried with air flow. In some cases the substrate was further treated by ultrasonification in acetone for 30 minutes, rinsed with demi water, then cleaned using UV-ozone equipment.

The PCBM-P3HT film (1:1) was spin-coated (1500 r.p.m.) on quartz from chloro-benzene (15 mg/ml P3HT). The film was annealed for 5 minutes at 140°C in vacuum.

The thickness of the film was determined to be 97 nm, with profilometry.

The film was prepared by Bram P. Karsten working in the group of Prof. R. A. J. Janssen at TU/e (Eindhoven). PCBM was obtained from Solenne ($> 99.5\%$) . RR-P3HT was obtained from Rieke Metals.

Spectroscopy

Absorption spectra were recorded on a single beam HP 8453 diode array spectrophotometer. The spectral range is from 190 nm to 1100 nm with a resolution of 2 nm. Fluorescence spectra were recorded on a SPEX Fluorolog 3-22 fluorimeter (with a Xe arc light source and a Hamamatsu R636-10 photomultiplier tube detector). The films were placed in an angle of ca. 56° to the emission channel to avoid reflection. The excitation and emission slits were ≤ 5 nm to reduce the effects of stray light.

Fluorescence spectra were corrected for the instrument response.

Femtosecond transient absorption (fs-TA) experiments were performed with a Spectra-Physics Hurricane Titanium:Sapphire regenerative amplifier system. The full spectrum setup was based on an optical parametric amplifier (Spectra-Physics OPA 800C) as the pump. The residual fundamental light, from the pump OPA, was used for white light generation, which was detected with a CCD spectrograph (Ocean Optics PC2000 + slave) for visible detection. The polarization of the pump light was controlled by a Berek Polarization Compensator (New Focus). The Berek Polarizer was always included in the setup to provide the magic-angle conditions. The probe light was double-passed over a delay line (Physik Instrumente, M-531DD) that provides an experimental time window of 3.6 ns with a maximum resolution of 0.6 fs/step. The OPA was used to generate excitation pulses at 550 nm (**PDI** excitation). The laser output was typically 2-3.5 μJ pulse⁻¹ (130 fs fwhm) with a repetition rate of 1 kHz. The overlap of pump and probe beams ($785 \times 10^3 \mu\text{m}^2$) was optimally aligned to be on the surface of each sample at the zero time. The focal point was ~ 10 cm after the sample. The film were kept in a nitrogen atmosphere during the measurements.

Layer thickness

The layer-thickness was estimated by using the density (ρ), the optical density (A), the molar absorption coefficient (ϵ) and the molar mass (M).

$$l = \frac{A}{\epsilon \frac{\rho}{M} \times 1000}$$

By using $\rho = 1.407 \text{ g cm}^{-3}$,

$\epsilon = 80\,000 \text{ l mol}^{-1}\text{cm}^{-1}$ (at 580 nm)

A = 0.8 (at 580 nm)

M = 944 mol g⁻¹

See:

Ramanan, C.; Smeigh, A. L.; Anthony, J. E.; Marks, T. J.; Wasielewski, M. R. *J. Am. Chem. Soc.* **2012**, *134*, 386– 397

Global and Target Analysis using Glotaran

The analysis of the time-resolved spectroscopic data consisting of a three dimensional dataset (wavelength, time and absorption difference intensity) was performed with the global and target analysis program GLOTARAN. <http://glotaran.org/>

After a first singular value decomposition of the raw data matrix, the starting number of components was estimated. From the first analyses with a sequential global model the chirp correction and the main decay/rise time constants were obtained. The number of components was further optimized. On the basis of the spectral shape (and experience) a target model was set up that contains branching from specific states. Then the ratios of this branching were introduced which influences mainly the amplitude of the species associated difference spectra (SADS), but not their shape or the decay/rise time constants. The most important spectral assumptions in the target analysis are the equality of the SADS of S_1 and $*S_1$ (red in Fig.6C) and the equality of the SADS of CT, $*CT$ and FCC (green in Fig.6C). In addition, we aimed for a similar bleach of the triplet SADS (cyan in Fig.6C) and the S_1 SADS near 450 nm, and for similar bleaches of the black, red and green SADS near 550 nm. Finally, a zero constraint was imposed on the triplet SADS above 710 nm.

In the final stage, analysis was performed with the more sophisticated and extended original UNIX source code on which Glotaran (and TIMP) are based.

Global analysis and Target analysis:

All spectra (measured at 256 wavelengths) were collated in a matrix, which was globally fitted using a sequential kinetic scheme with increasing lifetimes. From this the lifetimes and the EADS were estimated. The quality of the fit was judged by inspection of the singular vectors of the matrix of residuals, which had to be structureless. The instrument response function was described by a Gaussian shape, and the white-light dispersion over the spectral range was modelled as a second-order polynomial. With increasing lifetimes, and thus decreasing rates, the first of the EADS decays with the first lifetime and corresponds to the difference spectrum at time zero with an ideal, infinitely small instrument response function. The second of the EADS is formed with the first lifetime

and decays with the second lifetime. And so on. The error in the lifetimes obtained from the fitting procedure does not exceed 10%. EADS may not represent pure species, and they are interpreted as a weighted sum (with only positive contributions) of species-associated difference spectra (SADS).

To resolve the SADS from the EADS, a target analysis was performed on the data. In this target analysis, a kinetic scheme was used to estimate the microscopic rate constants and SADS of the different species.

The matrices of residuals resulting from the target analysis were further analysed using a singular value decomposition. The first left- and right singular vectors from show no or little structure, indicating that all kinetics are described satisfactorily.

For papers about Glotaran, see:

1. Mullen, K. M.; van Stokkum, I. H. M., TIMP: An R package for modeling multi-way spectroscopic measurements. *Journal of Statistical Software* 2007, 18 (3).
2. Snellenburg, J. J.; Laptinok, S. P.; Seger, R.; Mullen, K. M.; van Stokkum, I. H. M., Glotaran: a Java-based Graphical User Interface for the R-package TIMP. *Journal of Statistical Software* 2012, 49, 1-22.
3. van Stokkum, I. H. M.; Larsen, D. S.; van Grondelle, R., Global and target analysis of time-resolved spectra. *Biochimica Et Biophysica Acta* 2004, 1657, 82-104.

Target analysis of PDI only film

The global target analysis of the pure **PDI** film (without donor) is characterized by five excited state species, three of which have mainly singlet character. The fourth SADS has excimeric nature and the final, long-lived SADS has clear triplet state character. Similar observations were made for molecular dimeric species. ^{see 28k,l}

(Veldman, D.; Chopin, S. M. A.; Meskers, S. C. J.; Groeneveld, M. M.; Williams, R. M.; Janssen, R. A. J., Triplet formation involving a polar transition state in a well-defined intramolecular perylenediimide dimeric aggregate. *J. Phys. Chem. A* **2008**, *112*, 5846-5857. (l) Hippus, C.; van Stokkum, I. H. M.; Zangrando, E.; Williams, R. M.; Wykes, M.; Beljonne, D.; Wurthner, F., Ground- and excited-state pinched cone equilibria in calix[4]arenes bearing two perylene bisimide dyes. *J. Phys. Chem. C* **2008**, *112*, 14626-14638.)

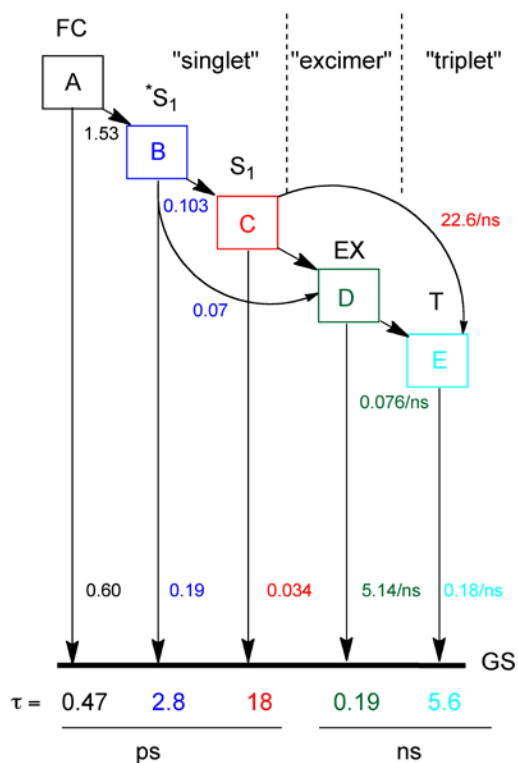


Figure S8. Target analysis scheme for the **PDI** film. Individual rates are indicated in ps⁻¹ or ns⁻¹ (when specified for the latter).

The kinetic scheme summarizes the target analysis findings. The FC excited state decays in ≈ 0.5 ps to a hot singlet *S1 (and to GS). In turn, *S1 decays to relaxed S1 (and to GS), and can also form the excimer. The final S1 decays to both GS and triplet. The excimer decays almost exclusively to GS.

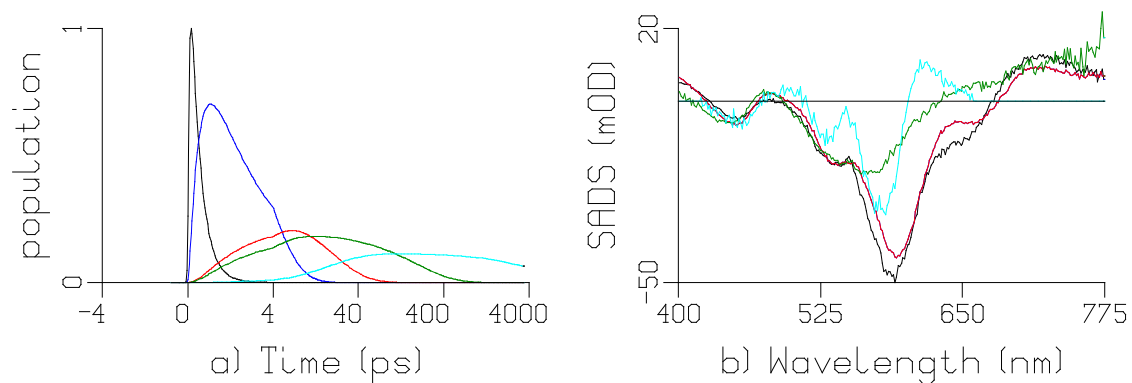


Figure S9

(a) (right) Population profiles of the excited state species. Key: black: FC, blue and red *S1 and S1 (*S1, S1 have the same SADS), dark green: excimer, cyan: T1. Time axis is linear from -4 till 4 ps, relative to the location of the IRF maximum, and logarithmic thereafter.

(b) (right) Species associated difference spectra (SADS).

The green SADS shows excited state dimer character (more pronounced and strong bleach band at ~ 530 nm (relative to 590 nm). Triplet spectrum is cyan color (light blue). In the model a spectral zero constraint was applied (for the triplet above 660 nm).

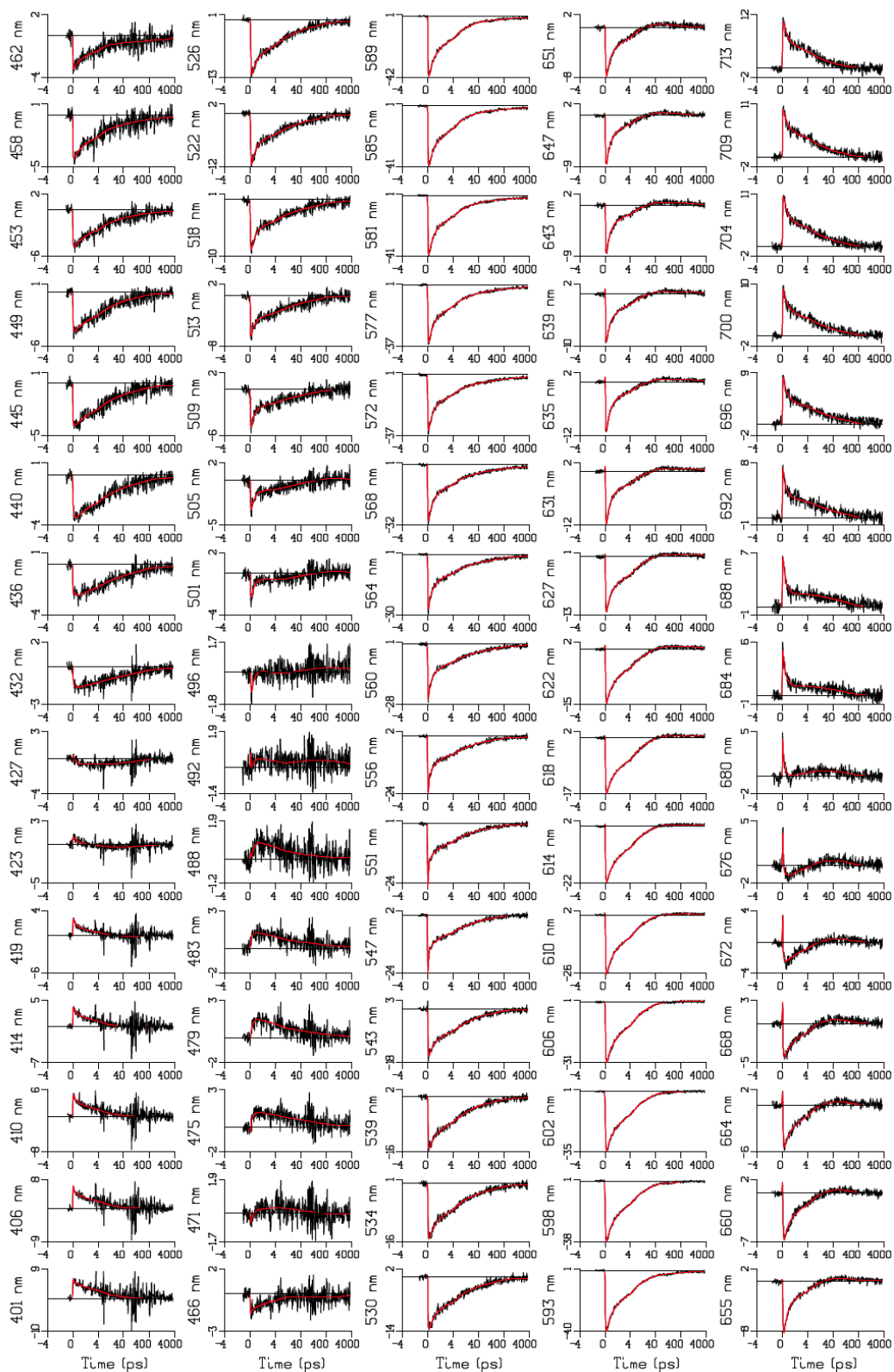


Figure S10. Kinetic traces with fit (at wavelength indicated) of the target analysis of the PDI film. Time axis is linear from -4 till 4 ps, relative to the location of the IRF maximum, and logarithmic thereafter.